Direct Inhibition of the mitochondrial permeability transition pore: A possible mechanism responsible for anti-apoptotic effects of melatonin

Article *in* The FASEB Journal · June 2004

DOI: 10.1096/fj.03-1031fje · Source: PubMed

5 authors, including:

Shaida Andrabi
University of Alabama at Birmingham
59 PUBLICATIONS **3,798** CITATIONS

SEE PROFILE

Iqbal Sayeed
Emory University
90 PUBLICATIONS **3,600** CITATIONS

SEE PROFILE

Gerald Wolf
Otto-von-Guericke-Universität Magdeburg
203 PUBLICATIONS **6,465** CITATIONS

SEE PROFILE

Thomas F.W. Horn
ETH Zurich
56 PUBLICATIONS **1,990** CITATIONS

SEE PROFILE

The FASEB Journal express article 10.1096/fj.03-1031fje. Published online March 19, 2004.

Direct inhibition of the mitochondrial permeability transition pore: a possible mechanism responsible for anti-apoptotic effects of melatonin

Shaida A. Andrabi,* Iqbal Sayeed,† Detlef Siemen,† Gerald Wolf,* and Thomas F. W. Horn*

[1]Institute for Medical Neurobiology and †Department of Neurology Otto-von-Guericke University, D-39120 Magdeburg, Germany

Corresponding author: T. F. W. Horn, Institute for Medical Neurobiology, Otto-von-Guericke, University Leipziger Str. 44, D-39120 Magdeburg, Germany. E-mail: thomas.horn@medizin.uni-magdeburg.de

ABSTRACT

Melatonin, the secretory product of the pineal gland, is known to be neuroprotective in cerebral ischemia, which is so far mostly attributed to its antioxidant properties. Here we show that melatonin directly inhibits the mitochondrial permeability transition pore (mtPTP). mtPTP contributes to the pathology of ischemia by releasing calcium and cytochrome c (cyt c) from mitochondria. Consistently, NMDA-induced calcium rises were diminished by melatonin in cultured mouse striatal neurons, similar to the pattern seen with cyclosporine A (CsA). When the mouse striatal neurons were subjected to oxygen-glucose deprivation (OGD), melatonin strongly prevented the OGD-induced loss of the mitochondrial membrane potential. To assess the direct effect of melatonin on the mtPTP activity at the single channel level, recordings from the inner mitochondrial membrane were obtained by a patch-clamp approach using rat liver mitoplasts. Melatonin strongly inhibited mtPTP currents in a dose-dependent manner with an IC_{50} of 0.8 μM. If melatonin is an inhibitor of the mtPTP, it should prevent mitochondrial cyt c release as seen in stroke models. Rats underwent middle cerebral artery occlusion (MCAO) for 2 h followed by reperfusion. Melatonin (10 mg/kg ip) or vehicle was given at the time of occlusion and at the time of reperfusion. Indeed, infarct area in the brain sections of melatonin-treated animals displayed a considerably decreased cyt c release along with less activation of caspase-3 and apoptotic DNA fragmentation. Melatonin treatment diminished the loss of neurons and decreased the infarct volume as compared with untreated MCAO rats. Our findings suggest that the direct inhibition of the mtPTP by melatonin may essentially contribute to its anti-apoptotic effects in transient brain ischemia.

Key words: patch clamp • intracellular calcium • TMRM • NMDA • apoptosis • fluo-4

Melatonin, the main secretory product of the pineal gland, is well known for its neuroprotective effects that are currently attributed mainly to its radical scavenging and antioxidant properties (1). It is highly effective in preventing neuronal loss in models of brain damage where oxidative stress is involved. The endogenous compound that readily crosses the blood-brain barrier (for review, see ref 1) was accordingly found to reduce the infarct size and neuronal injury in experimental ischemia (2-5). Furthermore, melatonin reduces

oxidative stress and rescues dopaminergic neurons in different models of Parkinson's disease (6, 7). Melatonin protects against the seizures induced by kainate, glutamate, and NMDA (8). Supporting the role of melatonin as an endogenous protectant, an aggravation of brain damage after ischemia or excitotoxic seizures have been reported in rats that are deficient in melatonin production (5). Besides the direct antioxidant potential, several other mechanisms such as interactions with calmodulin (9) are also considered to be involved in the melatonin-mediated neuroprotection. Melatonin is furthermore reported to directly alter the activities of detoxifying enzymes, thereby improving the total antioxidant defense capacity of the cells. Thus, systemic treatment with melatonin has been shown to cause an increase in the glutathione peroxidase activity in rats (10) as well as the gene expression of antioxidant enzymes including Mn-SOD, Cu/Zn-SOD (11). Moreover, melatonin prevents the activation of the transcription factor NF-κB (12). This may be the underlying mechanism by which melatonin reduces the expression of the inducible isoform of nitric oxide (NO) synthase (13), a major source of deleterious reactive nitrogen species like NO or its metabolite peroxynitrite. Recently, we demonstrated that NO contributes to high and potentially pro-apoptotic cytosolic calcium levels ($[Ca^{2+}]_c$) via an activation of the mitochondrial permeability transition pore (mtPTP), a megachannel formed in the mitochondrial membranes, resulting in a release of Ca^{2+} into the cytosol (14). The mtPTP is a complex found at the contact sites between the inner and outer mitochondrial membranes (15, 16). Under conditions like oxidative stress, high Ca^{2+}, and low ATP, a number of proteins including Bax and Bad are recruited that enable the pore formation at its high conductance state (15, 16). The complex, once it is formed, consists of several mitochondrial proteins, including voltage-dependent anion channels, adenine nucleotide translocase, and cyclophilin D (16, 17).

An intense stimulation of NMDA-type glutamate receptors results in a sustained elevation and deregulation of $[Ca^{2+}]_c$ (18, 19) that is triggered after the initiation of the mtPTP (20). Moreover, the mtPTP assembly that leads to cell death has been observed after deprivation of oxygen and nutrients in cell culture models (21), conditions that are accompanied by glutamate release and high $[Ca^{2+}]_c$ levels (22, 23). We showed that the NO-modulated mitochondrial calcium release via the mtPTP is a component of such NMDA-receptor mediated intracellular Ca^{2+} deregulation (14).

Our initial finding of the present study was that melatonin is able to reduce NMDA-induced high $[Ca^{2+}]_c$ levels in an almost identical pattern like cyclosporine A (CsA). CsA has proven to be protective in various models of cerebral ischemia in vitro and in vivo (24-26). These studies suggest that the inhibition of mtPTP activation comprises a target for pharmacological intervention to prevent cell death under conditions where this megachannel is formed. A mechanism of a direct mtPTP inhibition by melatonin would add to the explanation for its potent neuroprotective effect since mitochondria are now considered as the cellular relay stations that integrate various signals such as free radical production and $[Ca^{2+}]_c$, thereby deciding over life and death of the cell, besides their main function as the sites of respiration (27).

One of the early, potentially pathological mitochondrial responses to $[Ca^{2+}]_c$ overload that occurs due to excessive NMDA-receptor stimulation as seen, e.g., in cerebral ischemia, is the release of cytochrome c (cyt c). The released cyt c, along with apoptosis activating factor-1 (Apaf-1) and with ATP, activates caspase proteases via the apoptosome formation thereby triggering cellular self-destruction (28-30). Several mechanisms have been proposed for the release of cyt c into the cytosol. A large body of evidence suggests the mitochondrial permeability transition mediated by

the mtPTP is an underlying mechanism (16, 31). The mtPTP formation at its high conductance state releases cyt c and is accompanied by the loss of the mitochondrial membrane potential ($\Delta\psi_m$) that leads to ATP depletion and energetic collapse and hence contributes to the fate of the cell (32). A rupture of the outer mitochondrial membrane as a consequence of mitochondrial swelling due to the disturbed ionic homeostasis has been proposed as an alternative cyt c releasing mechanism that follows mtPTP formation (33).

The aim of this study is based on our initial finding in striatal neurons that melatonin inhibits the $[Ca^{2+}]_c$ rise after intense NMDA stimulation in a pattern similar to that of CsA. It raises the question if mtPTP inhibition is one of the mechanisms that mediates the neuroprotective effect of melatonin. To study the effect of melatonin on mtPTP activation, we investigated the direct effect of melatonin on the mtPTP by recording its activity at the single channel level employing a patch-clamp approach in mitoplasts. Following the hypothesis that an inhibition of the mtPTP by melatonin should also preserve the $\Delta\psi_m$, we studied the effect of melatonin in a neuronal cell culture model of ischemia where mtPTP formation is known to be associated with mitochondrial depolarization (34, 35). Consequently, one would assume that, being an mtPTP inhibitor, melatonin would also block the cyt c release after mtPTP formation as observed in cerebral ischemia. Therefore, we investigated the effect of melatonin on the cellular distribution of apoptotic markers, namely that of cyt c, caspase-3, and apoptotic-DNA fragmentation. For this purpose, we tested melatonin in a rat middle cerebral artery occlusion (MCAO) model of transient cerebral ischemia with reperfusion to further underline the effectiveness of melatonin as a neuro-protectant that involves mtPTP inhibition.

MATERIALS AND METHODS

Cell cultures

All animal protocols used in this study were in accordance with the Animal Health and Care Committee of the Land Sachsen-Anhalt, Germany. Cultures of embryonic mouse striatal neurons were prepared as described previously (14). In brief, striatal primordia from E15 mouse embryos were mechanically dissociated in growth media and plated onto 22 mm glass coverslips precoated with poly-L-lysine (1 mg/ml). Neurons were grown in serum-free Dulbecco's Modified Eagles Medium (DMEM, Sigma Chemicals, Deisenhofen, Germany) within a humidified atmosphere aerated with 5% CO_2 in air at 37°C and maintained for 7–8 days in vitro before experiments.

Intracellular Ca^{2+} measurements by fluo-4 imaging

Cell cultures were loaded with 2.5 μM fluo-4 AM (Molecular Probes, Leiden, Netherlands, stock solution prepared in DMSO and 20% pluronic acid) for 45 min at 37°C. After dye loading, the cultures were transferred into a stainless steel chamber (Atto-fluor, 2 ml volume) that was mounted on a thermostatically controlled stage (37°C) on an inverted confocal laser scanning microscope (AXIOVERT, LSM PASCAL, Zeiss, Germany). Cells were observed using a Zeiss x63 oil immersion lens. For imaging of Ca^{2+}-sensitive fluo-4 fluorescence, excitation light was provided by an argon laser at 488 nm. Fluo-4 fluorescence emission, filtered at 505 nm long-pass, was recorded using the photomultiplier of the LSM Pascal. Image acquisition frequency was set at 1 image per 10 s. Cells were superfused with HEPES-buffered salt solution (HBSS)

containing (in mM): 137 NaCl, 5 KCl, 20 HEPES, 10 glucose, 1.4 $CaCl_2$, 3 $NaHCO_3$, 0.6 Na_2HPO_4, 0.4 KH_2PO_4 at pH 7.4, at a rate of 2 ml/min using a peristaltic pump (Gilson). After the cells were mounted on the microscope, the cultures were superfused for 5 min with HBSS to wash out excess dye. Then the sequential imaging was started, and the cultures were further perfused with buffer alone for 100 s to obtain a steady baseline. Cultures were then subjected to a continuous application of 200 μM NMDA (Alexis Biochemicls, Grunberg, Germany). In two other subsets of experiments, either CsA (2 μM, Alexis Biochemicals) or melatonin (100 μM**,** Sigma Chemicals) was added to the superfusion buffer 20 s after the onset of the NMDA stimulation. Images from the cultures were collected for 20 min of the NMDA application. Analysis of fluorescence intensity was performed off-line after image acquisition by averaging intensity values within boxes overlying cell somata in the images using the imaging software of the Zeiss LSM. Data were normalized, and average image intensities were calculated.

Oxygen-glucose deprivation and mitochondrial depolarization

Cell cultures were subjected to 3 h oxygen-glucose deprivation (OGD) followed by 30 min reperfusion. For this purpose, the culture medium was removed and the cultures were washed with HBSS buffer to remove all the medium containing glucose. Then OGD was initiated by changing the medium of the cultures to glucose-free DMEM that was first bubbled for 20 min with a mixture of 5% CO_2 and the rest N_2 to remove O_2. The cultures were then immediately transferred into an incubator with a humidified hypoxic atmosphere containing 5% CO_2, 1% O_2 in N_2, maintained at 37°C. After 3 h, the OGD in the cultures was terminated by resupplying the glucose-containing DMEM and transferring them back into an incubator with a normal atmosphere containing 5% CO_2 in air.

For assessing the mitochondrial depolarization, the control and OGD-subjected cultures were incubated with 100 nM tetramethylrhodamine methylester (TMRM, Molecular Probes) at 37°C for 20-30 min. TMRM was added at time after the OGD termination. To test the effect on mitochondrial depolarization, either melatonin (100 μM) or CsA (2 μM) was added twice: at the time of OGD initiation as well as at the time of oxygen-glucose resupply. To image the TMRM fluorescence, excitation was set at 543 nm and emission was filtered at 570 nm long-pass and the filtered fluorescence light was recorded by photomultipliers. Within one set of experiments, gain and offset of the imaging program were kept constant. A very low laser intensity was used to avoid the photo activation of the dye.

Patch clamp of the mtPTP

To test the direct effect of melatonin on the mtPTP, we studied single-channel currents through the mtPTP by means of the patch-clamp techniques with mitoplasts, prepared from isolated liver mitochondria, applying different solutions by a flow system.

Preparation of mitoplasts

Livers of male Sprague-Dawley rats were cut in small pieces, homogenized by means of a teflon-pistle, and centrifuged for 5 min at 600 *g*. The resulting supernatant was centrifuged again for 4 min at 5100 *g*. The obtained pellet was resuspended in isolation medium containing 250 mM sucrose, 1 mM K-EDTA (pH 7.4), and centrifuged for 10 min at 12,300 *g*. The final pellet

containing the mitochondria was resuspended in storage medium and stored on ice for a maximum of 36 h. Mitoplasts were prepared by a hypoosmotic treatment with the hypotonic buffer containing, 5 mM K-HEPES, 0.2 mM $CaCl_2$ (pH 7.2). After a 1 min incubation at room temperature, the isotonicity was restored by addition of hypertonic medium: 750 mM KCl, 80 mM K-HEPES, 0.2 $CaCl_2$ mM (pH 7.2).

Electrophysiology

For patch-clamp experiments, borosilicate glass pipettes (Clark, Pangbourne, UK) were polished to yield resistances of 12-17 MΩ. Free-floating mitoplasts were approached by the pipette using an electrically driven micromanipulator. The mitoplasts were moved to their final position at the pipette tip by gentle suction. Gigaseals of ~1.5 GΩ were formed spontaneously or by additional suction. Experiments were done in the mitoplast-attached mode. Currents were recorded by an L/M-EPC-7 amplifier (HEKA electronics, Lambrecht, Germany). The currents were low-pass filtered by a 4-pole Bessel filter at a corner frequency of 0.5 kHz. Data were recorded at a sample frequency of 2.5 kHz by means of the pClamp software (Axon Instruments, Foster City, CA), which was also used for processing of the data. Melatonin in different concentrations (0.25, 0.8, 1, 10, 100 μM) was added through the glass capillaries of a peristaltic-pump driven flow system. Potentials given are measured at the inner side of the membrane. Inward currents are always depicted downwards in the traces. The probability that the channel is in an open state (P_o) was determined by an all points analysis according to the following equation:

$$P_o = \frac{(A_1 * B_1) + (A_2 * B_2) + ... + (A_n * B_n)}{B_{max}\,(A_0 + A_1 + A_2 + ... + A_n)}$$

where P_o is weighted by the different amplitudes of the substates (B_n) and A_n is the area under the Gaussian curves for the closed state and the different open states.

In vivo experiments

Animals

To test the effect of melatonin on mtPTP-induced apoptotic markers in the rat MCAO model, adult male Wistar rats weighing 300-350 g were used. The animals were kept under a 12-12 h light-dark cycle and were given free access to food and water. The rats were randomly divided into four treatment groups: “Sham + Vehicle” (injection of vehicle, no occlusion), “Sham + Mel” (rats treated with melatonin only, and no occlusion was performed), “MCAO + Vehicle” (MCAO was performed, and vehicle was given in place of the drug), and “MCAO + Mel” (MCAO was applied, and the animals were treated with melatonin).

Drug administration

Melatonin (10 mg/kg body weight in 10% ethanol) or the same volume of vehicle was administered in animals intraperitoneally twice: at the time of occlusion and at the time of reperfusion.

Surgical procedure

The animals were anesthetised with 2% halothane in 50% N_2O/50% O_2. During the whole surgical period, the body temperature of the animals was maintained at 36.5 ± 0.5 °C by the use of a heating pad, controlled by a rectal probe. Focal cerebral ischemia was induced by the intraluminal suture method (36) as modified by (37). Briefly, a 3-0 nylon suture (Ethicon, Johnsons & Johnsons Intl, Brussels, Belgium) with its tip rounded by heating near a flame and coated with poly-L-lysine was introduced into the internal carotid artery through a nick in the external carotid artery and advanced 17-20 mm from the common carotid artery bifurcation to block the origin of middle cerebral artery (MCA). The suture was left in place for 2 h while the animals were allowed to wake up. After 2 h of occlusion, the intraluminal suture was gently removed during a brief period of anesthesia to allow reperfusion. In the groups of sham-operated rats ("Sham + vehicle" and "Sham + Mel"), all surgical procedures except the occlusion of the MCA were performed. The animals were then returned to their cages and given free access to food and water.

Immunohistochemistry

For evaluation of the apoptotic cascade, cytosolic changes in cyt c and caspase-3 were investigated, using immunohistochemical studies at the 4 and 24 h time points after reperfusion. Along with cyt c and caspase-3, MAP-2 and NeuN, markers for neuronal degeneration were also studied. Subsets of four animals in each group were deeply anaesthetized with mixture of Domitor and ketamine hydrochloride and were transcardially perfused with 100 ml of saline followed by 300 ml of 4% paraformaldehyde (PFA) and 0.2% glutaraldehyde in PBS. After postfixation in 4% PFA, the brains were cryoprotected in 0.5 M sucrose for 24 h followed by 1.0 M sucrose for 72 h at 4°C. Thereafter, the brains were cut into 25 μm thick coronal sections, and the free floating sections were rinsed with PBS and then incubated in blocking buffer (10% fetal calf serum in PBS with 0.3% Triton X-100) at room temperature for 1 h to block nonspecific binding sites. The sections were then incubated with the primary antibodies (diluted in PBS with 0.3% Triton X-100 and 1% calf serum) overnight at 4 °C. The following antibodies were used: rabbit anti-cytochrome c, 1:200 (Santa Cruz Biotechnology); rabbit anti-caspase 3, 1:200 (Santa Cruz Biotechnology); monoclonal anti-MAP 2, 1:1000 (Sternberger); and anti-NeuN, 1:500 (Chemicon). Primary antibody binding was detected by incubating the sections with fluorescent conjugated anti-rabbit (1:500, Alexa 546, Molecular Probes) or anti-mouse (1:500, Alexa 546, Molecular Probes) secondary antibodies (diluted in PBS) for 2 h at room temperature. In control sections, the buffer was added instead of primary antiserum. LSM Pascal confocal microscope (Carl Zeiss) was used for visualisation of the immunostained sections.

For assessing the apoptotic DNA fragmentation, a monoclonal antibody (Apostain, Alexis Biochemicals) was used. The apostain method was followed as provided by the manufacturer with some modifications. Briefly, the perfusion fixed brains with 4% PFA were postfixed in the same fixative for 24 h and thereafter cut into 25 μm thick frozen sections. The sections were taken up onto the superfrost slides and heated in 50% formamide to yield single stranded DNA (ssDNA) fragments. The slides were then incubated with the monoclonal antibody to ssDNA (1:50) for 30 min at 37 °C to label the ssDNA fragments. The primary antibody binding was detected by incubating the sections with horse-radish peroxidase-conjugated IgM rat monoclonal anti-mouse secondary antibody (Zymed, diluted 1:50 in PBS) and counterstained with

hematoxyline. The darkly-stained apoptotic cells were visualized in transmission light mode using the LSM Pascal confocal microscope (Carl Zeiss).

All the investigations were carried out in the ischemic cortical region (see Results) in the section taken at the level approximately 2 mm posterior to bregma.

Infarct assessment

To verify the neuroprotective effect of melatonin, the animals (n=10 for each group) were euthanised 3 days after reperfusion, under halothane anesthesia followed by decapitation. The brains were rapidly dissected out, and the forebrains were cut into six 2-mm thick coronal sections using a rat brain matrix (Activational Systems Inc.). The sections were stained by incubating them in a solution of 2% 2, 3, 5-triphenyltetrazolium chloride (TTC) at 37 °C for 15 min and then fixed in 10% buffered PFA. For imaging, the sections were scanned after 24 h by a high resolution scanner (Hewlett Packard Scanjet 6100C/T). The total mean infarct area of each section was calculated as the average of the area on the rostral and the caudal side. The total area was calculated by adding the average area from each section. Multiplication of the total area by 2 mm (thickness of the sections) was calculated as infarct volume, expressed in mm^3.

Statistical analysis

Data are means ± SE. For statistical analysis of the infarct volume, one-way analysis of varience (ANOVA) was applied followed by Dunnett's Multiple Comparison test. For the results obtained with NMDA-induced $[Ca^{2+}]_c$ rise, data were collapsed at every 100 s time point after onset of NMDA application. These data were then treated with two-way ANOVA followed by Tukey's t test. *$P < 0.05$ was considered to be statistically significant.

RESULTS

Melatonin reduced the sustained $[Ca^{2+}]_c$ increase in primary neuronal cultures exposed to NMDA

We first studied if melatonin modulates the NMDA-induced $[Ca^{2+}]_c$ rises as measured by fluo-4 confocal imaging in mouse striatal neurons. Upon stimulation of striatal neurons with 200 μM NMDA, we observed a fast initial increase in the fluo-4 fluorescence from a baseline intensity of 103.4 ± 4.3 (average of single cell arbitrary intensity values ± SE, n=5 cultures) to a level of 282.3 ± 22.5 immediately after exposure to NMDA (Fig. 1). The increased fluorescence, indicating an increase in $[Ca^{2+}]_c$, did not return to the baseline level but remained at a sustained plateau level for the whole experiment. After 18 min of NMDA application, the fluorescence was still high at 284.3 ± 16.2.

When CsA (2 μM) was added to the NMDA-containing superfusion solution, the neurons exhibited again a fast initial increase in the fluorescence, peaking at similar levels (297.3±7.2, n=5 cultures). However, the fluo-4 fluorescence did not remain at the plateau levels with CsA treatment and instead started to decline (Fig. 1). At 5 min of CsA + NMDA application, a significant decrease in the NMDA-induced sustained fluorescence was observed (207.7±15.2, P<0.05) and at 18 min of CsA application the values declined to 188.8 ± 23.0 (P<0.05). When

melatonin (100 μM) was added to the NMDA-containing superfusion solution, the fluorescence plateau started to decline again in a similar pattern as seen with CsA (Fig. 1). At 5 min of melatonin + NMDA application, the fluorescence values significantly decreased from 281.9 ± 12.6 to 230.3 ± 14.7 ($P<0.05$) and at 18 min of melatonin application to 181.5 ± 11.9 ($P<0.05$).

Melatonin inhibited the mtPTP

We investigated if melatonin has a direct inhibitory effect on the mtPTP. For that purpose, we recorded the mtPTP channel currents from patches of the inner mitochondrial membrane. The recordings displayed a characteristic activity of the mtPTP with an extremely large single channel conductance of more than 1 nS and a large variety of subconductance states that could all be reversibly blocked by 1 μM CsA, (Fig. 2*A*) as described before (38). Melatonin inhibited the P_o of mtPTP (Fig. 2*C*) in a dose-dependent manner ranging from 250 nM to 100 μM. The respective concentration response relation is shown in Fig. 3*C*. The best fit by means of the Hill equation was calculated with an IC_{50} of 0.8 μM and a Hill coefficient of 1. A maximum decrease in the P_o by only 20% reflects the fact that the effect of melatonin even at higher concentration is gradual and as the initial records also contribute to the mean P_o, the mean values do not decline to zero, instead saturate at 80% (P_o/P_o max = 0.2). This effect was reversible upon washout in the control solution (Fig. 2*B*, 4th trace).

Melatonin prevented mitochondrial depolarisation after OGD in primary neuronal cultures

We used the potentiometric fluorescent dye TMRM to monitor its uptake in OGD-subjected mouse striatal neurons in the presence or absence of CsA or melatonin as a measure for the integrity of the $\Delta\psi_m$. Fluorescence images of TMRM-incubated cultures, obtained after 3 h of OGD and 30 min glucose-oxygen resupply, showed only little TMRM fluorescence in mitochondria-like structures, an indication that the mitochondria were largely depolarized after the insult (Fig. 2*Db*). The few structures that exhibited a TMRM fluorescence displayed an unusual round short shape whereas the mitochondria-like structures in control cultures that did not undergo the OGD procedure showed an intensive fluorescence (Fig. 2*Da*). When the OGD-subjected cultures were additionally treated with 2 μM CsA,the loss of TMRM-labeled mitochondria-like structures was partially reversed (Fig. 2*De*). Similarly, a treatment with 100 μM melatonin prevented the loss of TMRM uptake due to OGD. The mitochondrial shape was less disrupted in these cultures (Fig. 2*Dc*). Melatonin or CsA per se did not alter the TMRM uptake into the neurons that were not subjected to OGD (Fig. 2*Dd*). Furthermore, we tested the TMRM-uptake into the mitochondria in control cultures that were treated with Verapamil (5 μM) 5 min before TMRM incubation to inhibit the multidrug resistance pump (MDR). We found that the TMRM-uptake in verapamil treated cultures was not different from that of control cultures, treated with either vehicle, melatonin, or CsA (data not shown).

Anti-apoptotic effects of melatonin in the MCAO model of cerebral ischemia

Melatonin prevented the release of cyt c release from mitochondria

We explored the effect of melatonin treatment on the cytosolic cyt c immunoreactivity in brain sections of the infarct area in MCAO rats, using immunohistochemistry. MCAO followed by

reperfusion in the "MCAO + Vehicle" group caused a pronounced increase in the cytosolic cyt c immunoreactivity at 4 h as well as 24 h after the reperfusion (Fig. 3*A*). At 4 h, the cytosol was strongly stained for cyt c immunoreactivity. At 24 h after reperfusion, the cyt c immunoreactivity extended even to the intercellular space (Fig. 3*A*) indicating massive degeneration of the cells and shedding-off the intracellular contents into the intercellular spaces. In contrast, the "Sham + Vehicle" rats showed a profile cyt c staining at both 4 h as well as 24 h (Fig. 3*A*) that was indicative of intact mitochondria. When MCAO-subjected animals were treated with melatonin "MCAO + Mel," the cytosolic cyt c immunostaining as well as the intercellular cyt c staining signals decreased both at 4 has well as 24 h (Fig. 3*A*).

Melatonin prevented caspase-3 activation

At 4 h of occlusion, sections of "MCAO + Vehicle" rats showed a massive activation of caspase-3 in the ischemic cortex as compared with the "Sham + Vehicle" rats (Fig. 3*B*) that was still detectable at 24 h after reperfusion but not localized in well-defined cellular compartments (Fig. 3*B*). Upon melatonin treatment, the caspase-3 activation was drastically reduced in "MCAO + Mel" rats both at 4 h and 24 h (Fig. 3*B*). No changes in caspase-3 staining were observed in "Sham + Mel" rats when compared with "Sham + Vehicle" rats.

Melatonin reduced apoptotic DNA fragmentation

In "MCAO + Vehicle" rats, the apostain label was observed in the nuclei of a large cell population. Such apostain-positive cells showed a characteristic morphology of apoptotic cells with shrunken structures. The number of apostain-positive cells was reduced by melatonin in "MCAO + Mel" rats (Fig. 3*C*), showing an anti-apoptotic effect of melatonin.

Melatonin reduced the MCAO-induced brain damage

Decrease in the infarct volume

TTC staining of brain slices obtained from "MCAO + Vehicle" rats showed reproducible and readily detectable lesions in the areas that are supplied by MCA, at 3 days after the reperfusion (Fig. 4*A1*). The lesions were present both in the lateral striatum and the overlying cortex.

Melatonin, when given at the onset of occlusion and reperfusion in "MCAO + Mel" rats, reduced significantly the infarct volume to 147.0 ± 10.4 mm^3 ($P<0.05$, $n=10$), as compared with "MCAO + Vehicle" rats (290.0±13.5 mm^3, $n=10$, Fig. 4*A2*).

Prevention of the loss of MAP-2 and NeuN staining in the ischemic tissue

To elucidate at the cellular level, the extent to which neurons are protected in melatonin-treated MCAO rats, we studied the changes in MAP-2 and NeuN immunoreactivity in the cortical infarct area. In the "Sham + Vehicle" rats, the MAP-2 staining was characterized by a uniformly strong fluorescence of both dendrites and soma (Fig. 4*B*). After 24 h of reperfusion, a pronounced loss of MAP-2 staining (Fig. 4*B*) was observed in the "MCAO + Vehicle" group, whereby some localized beaded pattern of immunoreactive structures remained. After melatonin treatment "MCAO + Mel," the MAP-2 staining was preserved both in the dendritic arbour and soma in the ischemic cortex of "MCAO + Mel" rats at 24 h after reperfusion (Fig. 4*B*).

A well-defined NeuN staining was observed in "Sham + Vehicle" rats. In contrast, the NeuN-positive cells were almost completely lost from the ischemic cortex in "MCAO + Vehicle" rats at 24 h after the start of reperfusion (Fig. 4*B*), indicating a massive neuronal degeneration. Melatonin treatment greatly prevented the loss of NeuN-positive cells after 24 h of reperfusion in "MCAO + Mel" rats.

DISCUSSION

We were prompted to consider an action of melatonin on the mtPTP pathway by the initial observation that melatonin decreased the NMDA-induced sustained $[Ca^{2+}]_c$ plateaus. Such elevated $[Ca^{2+}]_c$ during continuous NMDA application is a result of Ca^{2+} influx and internal trafficking of the Ca^{2+} load whereby endoplasmic and mitochondrial Ca^{2+} uptake as well as Ca^{2+} release from these sites plays a role. The mitochondria act as Ca^{2+} buffers by sequestering excess Ca^{2+} from the cytosol. The $[Ca^{2+}]_c$ continues to rise when NMDA receptors are continuously stimulated causing Ca^{2+} uptake into the mitochondria that upon reaching a threshold level leads to mtPTP opening, which in turn produces Ca^{2+}-induced Ca^{2+} release (39). The mitochondrial permeability transition, allowing the nonselective permeation of ions and solutes through the mitochondrial membrane, is CsA sensitive (40, 41). Indeed, our experiments, using CsA at a low concentration that is primarily known to block the mtPTP (39), lowered the NMDA-induced $[Ca^{2+}]_c$ levels. This effect indicates the presence of a mtPTP-mediated Ca^{2+} release that contributes to the overall $[Ca^{2+}]_c$ in our cell culture model.

Melatonin, when used analogous to the CsA treatment, showed in our experiments an almost identical pattern in reducing the NMDA-induced $[Ca^{2+}]_c$ levels as seen with CsA. Such observation would indicate either a direct effect of melatonin on the mtPTP or on mechanisms upstream of mtPTP activation. One of such upstream factors is excessive free radical levels that may also lead to an mtPTP induction. Indeed, we showed earlier that the NMDA-induced $[Ca^{2+}]_c$ rises possess a component that is due to mtPTP activation by NO (14). Taking into account that melatonin is an excellent radical scavenger and antioxidant (1) one would assume that the observed effect on $[Ca^{2+}]_c$ after NMDA is due to the removal of NO or other reactive oxygen species that are believed to lead to the pathological mtPTP formation (42).

However, we show here that another mechanism, the observed direct inhibition of the mtPTP, is likely to contribute also to this effect. The mtPTP patches obtained from mitoplasts derived from liver mitochondria showed the characteristically voltage dependence and large conductance of >1 nS (38). The observed blockade of mtPTP currents by CsA application to the mitochondrial membrane patches together with the earlier shown Ca^{2+}-dependence indicate that the investigated megachannel was indeed the mtPTP. Comparability of mtPTP behavior in mitoplasts with observations made using O_2 measurements or a swelling assay (43) make it unlikely that the osmotic shock could have unpredictably altered the behavior of the mtPTP. As the patches were prepared at high Ca^{2+} concentration, mostly fully open mtPTPs were detected at the time of experiment. This comprises an advantage for the patch-clamp technique because potentially mtPTP-modulating factors like free radicals, which are effective upstream of the direct interactions with the channel, are excluded. Hence, the observed dose-dependent reduction in the pore currents due to bath application of melatonin is solely due to a direct interaction of melatonin with the channel. Our data show that the efficacy of melatonin in inhibiting the mtPTP is high with an IC_{50} of 0.8 μM. The inhibitory effect started quickly at 10 s after the addition of

melatonin to the patch-clamp bath solution, and the effect was seen even at very low concentrations (250 nM). In the light of the well-known reducing capacity of melatonin, one could speculate that a direct action on the mtPTP is possibly a common feature of antioxidants. However, preliminary results in our laboratory using the polyphenolic hydroxystilbene oxyresveratrol show that this antioxidant (44) failed to block mtPTP currents.

Previous studies using various other mtPTP blocking agents show that in pathological conditions such as ischemia an excessive loading of Ca^{2+} into the mitochondria induces apoptosis by stimulating the release of apoptosis-promoting factors like cyt c, AIF, Smac/DiaBLO, and procaspases from the mitochondrial intermembrane space into the cytoplasm via a permeability transition mechanisms (45). The release mechanism is believed to be accompanied by mitochondrial depolarization that follows the mitochondrial permeability transition. Hence, one would assume that melatonin, being an mtPTP blocker, may preserve $\Delta\Psi_m$ in ischemic conditions. To test this assumption, we used an OGD model of neuronal cultures in conjunction with live cell imaging of the fluorescent dye TMRM that is selectively taken up in energized mitochondria. As expected, we found that the TMRM uptake in OGD-subjected cultures was strongly compromised compared with control cultures, indicating that the noxious OGD stimulus leads to a decrease in $\Delta\psi_m$ as previously reported (46). The protection against the OGD-induced loss of TMRM-uptake by CsA in our OGD model indicates the involvement of the mtPTP in the mitochondrial depolarization. Indeed, melatonin also prevented the loss in TMRM uptake, which in turn reflects the preservation of $\Delta\psi_m$. The TMRM uptake was not altered by melatonin in control cultures that were not subjected to OGD, indicating that melatonin exerts its effect only when pathological conditions like mtPTP formation prevail. It has been shown that CsA in addition to its effect on the mtPTP has the potential to inhibit also the MDR. This may cause changes in attaining the mitochondrial TMRM fluorescence in the cells that is independent of mtPTP action (for review see ref 31). Previously, it was shown that that the MDR inhibition by verapamil, that is also an MDR inhibitor, did not cause any alteration in the CsA-induced mitochondrial hyperpolarization (47). If the component of MDR inhibition plays a role in our experimental model, one would assume that a treatment with verapamil results in a higher mitochondrial TMRM-uptake. Our results show that MDR inhibition by verapamil did not produce any change in attaining the mitochondrial TMRM uptake. Furthermore, using different concentrations (50-200 nM, concentrations that are below the self-quenching threshold) of TMRM showed no changes in mitochondrial fluorescence (data not shown), indicating that an increased intracellular availability of TMRM, as would result from a MDR blockade, does not alter the baseline fluorescence in our model. Thus, our results show that a possible MDR inhibition in our model does not affect the mitochondrial TMRM uptake using our loading protocol. A large body of evidence suggests that the mtPTP is causally involved in the pathological changes after ischemia/reperfusion (15, 48). Hence, a blockade of the mtPTP by melatonin may comprise a pharmacological strategy for the treatment of such pathological conditions. During ischemia, the ATP level drops and the concentration of ADP and AMP increases due to the cessation of the mitochondrial oxidative phosphorylation (49). Furthermore, tissue acidosis occurs during ischemia due to lactate accumulation (50). Adenine nucleotides and low pH are potent blockers of the mtPTP (51); therefore, it is unlikely that mtPTP opening occurs during the occlusion phase of stroke. Also, the uptake of cytosolic Ca^{2+} into mitochondria, being a prerequisite for mtPTP formation, is prevented by the mitochondrial depolarization that is initiated soon after the onset of the occlusion. However, during reperfusion,

mitochondria become re-energized; hence, the sequestration of Ca^{2+} that gets accumulated in the cytosol during ischemia (52) is reinstated. In addition, a shift toward a higher pH and excessive free radical generation has to be expected under such conditions (53, 54). All these factors that occur during reperfusion favor the mtPTP formation. Accordingly, mitochondrial swelling as a result of permeability transition is observed in neurons within the first hours of reperfusion (55). Taking into consideration that the reperfusion phase after ischemia is essential for the mtPTP opening, we choose to examine the effect of melatonin on the pathological changes in an MCAO model with 2 h occlusion followed by reperfusion. mtPTP-mediated brain injury has already been characterized in this MCAO model (56), and it was shown before that CsA treatment is protective in similar models of brain ischemia (24, 26). Since CsA also inhibits calcineurin, one could assume that CsA may act as a protectant at least in part by using this pathway. In most of these studies, the neuroprotective effect of CsA was observed to be much more efficacious than that of FK506, an immunosuppressant that has an ability to inhibit calcineurin like CsA but has no effect of mtPTP. Moreover, *N*-methyl-valine-4-cyclosporine A (MeValCsA), a CsA analog that has no effect on calcineurin but blocks the mtPTP opening, has been shown to decrease the infarct volume in the MCAO model to the same extent as seen with CsA (57).

We used cyt c immunoreactivity in the cytosol as a marker for mtPTP activation in our MCAO model. It was shown before that such ischemia-induced cyt c release is blocked by CsA (58) indicating a mtPTP-dependent mechanism. Consistently, we also observed high levels of cyt c immunoreactivity in the brain cytosol of MCAO-subjected rats at 4 h as well as at 24 h after the onset of reperfusion. We then proved our hypothesis that melatonin treatment reduces this increase in cytosolic cyt c immunoreactivity too, suggesting a lower mtPTP activity in presence of the drug. Such mtPTP-mediated cyt c release appears to be a feature also of other neuropathologies: CsA reduced the cyt c release from mitochondria in kainate-induced excitotoxicity in organotypic hippocampal cultures (59) and in neurons exposed to transient hypoglycemia (60). Isolated brain mitochondria were shown to release cyt c in a mtPTP-dependent mechanism when subjected to high Zn^{2+} levels (61) or to the neurotoxin MPP^{+} used in experimental Parkinson models (62).

Some contradicting studies on isolated mitochondria suggest that the release of cyt c might occur also independently of the mtPTP. For example, Andreyev and Fiskum (63) showed that mtPTP-mediated cyt c release was found in liver but not in brain mitochondria suspensions. The discrepancy between these studies is not fully understood. It was suggested that the induction of mtPTP opening and subsequent cyt c release from brain mitochondria might require the intact tissue (63).

We followed the cascade of events that extends downstream from the mtPTP-mediated cyt c release by examining how melatonin affects the caspase-3 activation (60) and the subsequent DNA fragmentation (64). Our MCAO model displayed an activation of caspase-3 that was inhibited by melatonin consequentially also prevented the DNA fragmentation.

The melatonin-induced anti-apoptotic effects presented here are in agreement with other studies showing that melatonin inhibits apoptosis in ischemic kidney (65) and in amyloid β-peptide injury in hippocampal neurons (66) and NO-induced cell death in PGT-β immortalized pineal cells (67). It is interesting to note that melatonin is not protective in all models of apoptotic cell death (68), which may find its explanation in the fact that all the investigated noxious stimuli do

not trigger mtPTP-mediated apoptotic pathways. For example, melatonin does not protect against staurosporine-induced apoptosis, which is known to follow pathways that do not involve mitochondrial depolarization; hence, the mtPTP is unlikely to be involved (69, 70).

Our in vivo data do not rule out additionally to the direct mtPTP inhibition, an indirect effect of melatonin on the mtPTP activation by removing reactive nitrogen or oxygen species from the tissue. The clearly observed in vitro actions of melatonin directly on the mtPTP may rather contribute to the overall outcome of its protective effect in in vivo stroke models. The finding of a reduction in the infarct volume in our studies is in agreement with previous results obtained by different authors that melatonin reduces the infarct size after cerebral ischemia (2-5) and serves here as a control for effectiveness of the MCAO insult.

The dose used in the present study is a pharmacological dose that has already been shown to cause neuroprotection in different models of neuronal degeneration (4, 71, 72). The relevance of physiological melatonin levels in inhibiting brain damage due to ischemia/reperfusion in rats was confirmed by Kilic et al. (73). They showed that physiological melatonin concentrations are neuroprotective and also the pharmacological application effectively reduces the brain damage and improves the neurological status of ischemic rats. The findings that physiological melatonin concentrations are neuroprotective are of particular interest since endogenous levels of melatonin are diminished in many aged individuals (74). Thus, elderly individuals may be increasingly vulnerable to the damaging effects of a stroke because they lack the endogenous protectant melatonin. Melatonin is well known to modulate the activities of hypothalamic centers that regulate the circadian rhythm. Diurnal modulations of Ca^{2+} currents in the suprachiasmatic nucleus of the hypothalamus are reported to transduce the intracellular cycling of molecular clocks and circadian rhythm (75). Since the mtPTP at its low-conductance state plays a role in the regulation of cellular Ca^{2+} homeostasis (39), one may speculate in the context of our findings that melatonin could modulate such pathways. The results of the present study therefore open a new field for investigating other regulatory principles in melatonin controlled mechanisms. Taken together, our results demonstrate for the first time that melatonin directly inhibits the mtPTP and that this effect may contribute to the anti-apoptotic properties of melatonin. The direct inhibition of mtPTP provides an evidence for an alternative mechanism that is used by melatonin to offer neuroprotection. Being an antioxidant and inhibitor of the mtPTP, therapeutic intervention by melatonin may provide beneficial clinical applications for the treatment of stroke and neurodegenerative disorders. Since melatonin is safe and nontoxic, more experimental studies should be conducted to explore the synergetic actions of melatonin with other drugs that are presently applied clinically.

ACKNOWLEDGMENTS

Technical assistance of Heike Baumann is gratefully appreciated. This work is supported by the grants DFG WO 474/11-4 and Sachsen Anhalt Grant 2997A/088G, 3496A/0203M, and NBL3 01220107.

REFERENCES

1. Tan, D. X., Manchester, L. C., Reiter, R. J., Qi, W. B., Karbownik, M., and Calvo, J. R. (2000) Significance of melatonin in antioxidative defense system: reactions and products. *Biol. Signals Recept.* **9,** 137-159

2. Pei, Z., Pang, S. F., and Cheung, R. T. (2002) Pretreatment with melatonin reduces volume of cerebral infarction in a rat middle cerebral artery occlusion stroke model. *J. Pineal Res.* **32,** 168-172

3. Pei, Z., Pang, S. F., and Cheung, R. T. (2003) Administration of melatonin after onset of ischemia reduces the volume of cerebral infarction in a rat middle cerebral artery occlusion stroke model. *Stroke* **34,** 770-775

4. Cho, S., Joh, T. H., Baik, H. H., Dibinis, C., and Volpe, B. T. (1997) Melatonin administration protects CA1 hippocampal neurons after transient forebrain ischemia in rats. *Brain Res.* **755,** 335-338

5. Manev, H., Uz, T., Kharlamov, A., and Joo, J. Y. (1996) Increased brain damage after stroke or excitotoxic seizures in melatonin-deficient rats. *FASEB J.* **10,** 1546-1551

6. Joo, W. S., Jin, B. K., Park, C. W., Maeng, S. H., and Kim, Y. S. (1998) Melatonin increases striatal dopaminergic function in 6-OHDA-lesioned rats. *Neuroreport* **9,** 4123-4126

7. Acuna-Castroviejo, D., Coto-Montes, A., Gaia Monti, M., Ortiz, G. G., and Reiter, R. J. (1997) Melatonin is protective against MPTP-induced striatal and hippocampal lesions. *Life Sci.* **60,** PL23-29

8. Lapin, I. P., Mirzaev, S. M., Ryzov, I. V., and Oxenkrug, G. F. (1998) Anticonvulsant activity of melatonin against seizures induced by quinolinate, kainate, glutamate, NMDA, and pentylenetetrazole in mice. *J. Pineal Res.* **24,** 215-218

9. Huerto-Delgadillo, L., Anton-Tay, F., and Benitez-King, G. (1994) Effects of melatonin on microtubule assembly depend on hormone concentration: role of melatonin as a calmodulin antagonist. *J. Pineal Res.* **17,** 55-62

10. Barlow-Walden, L. R., Reiter, R. J., Abe, M., Pablos, M., Menendez-Pelaez, A., Chen, L. D., and Poeggeler, B. (1995) Melatonin stimulates brain glutathione peroxidase activity. *Neurochem. Int.* **26,** 497-502

11. Antolin, I., Rodriguez, C., Sainz, R. M., Mayo, J. C., Uria, H., Kotler, M. L., Rodriguez-Colunga, M. J., Tolivia, D., and Menendez-Pelaez, A. (1996) Neurohormone melatonin prevents cell damage: effect on gene expression for antioxidant enzymes. *FASEB J.* **10,** 882-890

12. Mohan, N., Sadeghi, K., Reiter, R. J., and Meltz, M. L. (1995) The neurohormone melatonin inhibits cytokine, mitogen and ionizing radiation induced NF-kappa B. *Biochem. Mol. Biol. Int.* **37,** 1063-1070

13. Gilad, E., Wong, H. R., Zingarelli, B., Virag, L., O'Connor, M., Salzman, A. L., and Szabo, C. (1998) Melatonin inhibits expression of the inducible isoform of nitric oxide synthase in murine macrophages: role of inhibition of NFkappaB activation. *FASEB J.* **12,** 685-693

14. Horn, T. F., Wolf, G., Duffy, S., Weiss, S., Keilhoff, G., and MacVicar, B. A. (2002) Nitric oxide promotes intracellular calcium release from mitochondria in striatal neurons. *FASEB J.* **16,** 1611-1622

15. Crompton, M. (1999) The mitochondrial permeability transition pore and its role in cell death. *Biochem. J.* **341,** 233-249

16. Kroemer, G., and Reed, J. C. (2000) Mitochondrial control of cell death. *Nat. Med.* **6,** 513-519

17. Crompton, M. (2000) Mitochondrial intermembrane junctional complexes and their role in cell death. *J. Physiol.* **529,** 11-21

18. Peng, T. I., Jou, M. J., Sheu, S. S., and Greenamyre, J. T. (1998) Visualization of NMDA receptor-induced mitochondrial calcium accumulation in striatal neurons. *Exp. Neurol.* **149,** 1-12

19. Nicholls, D. G., and Budd, S. L. (2000) Mitochondria and neuronal survival. *Physiol. Rev.* **80,** 315-360

20. Alano, C. C., Beutner, G., Dirksen, R. T., Gross, R. A., and Sheu, S. S. (2002) Mitochondrial permeability transition and calcium dynamics in striatal neurons upon intense NMDA receptor activation. *J. Neurochem.* **80,** 531-538

21. Khaspekov, L., Friberg, H., Halestrap, A., Viktorov, I., and Wieloch, T. (1999) Cyclosporin A and its nonimmunosuppressive analogue N-Me-Val-4-cyclosporin A mitigate glucose/oxygen deprivation-induced damage to rat cultured hippocampal neurons. *Eur. J. Neurosci.* **11,** 3194-3198

22. Goldberg, M. P., and Choi, D. W. (1993) Combined oxygen and glucose deprivation in cortical cell culture: calcium-dependent and calcium-independent mechanisms of neuronal injury. *J. Neurosci.* **13,** 3510-3524

23. Goldberg, M. P., Weiss, J. H., Pham, P. C., and Choi, D. W. (1987) N-methyl-D-aspartate receptors mediate hypoxic neuronal injury in cortical culture. *J. Pharmacol. Exp. Ther.* **243,** 784-791

24. Uchino, H., Minamikawa-Tachino, R., Kristian, T., Perkins, G., Narazaki, M., Siesjo, B. K., and Shibasaki, F. (2002) Differential neuroprotection by cyclosporin A and FK506 following ischemia corresponds with differing abilities to inhibit calcineurin and the mitochondrial permeability transition. *Neurobiol Dis.* **10,** 219-233

25. Uchino, H., Elmer, E., Uchino, K., Li, P. A., He, Q. P., Smith, M. L., and Siesjo, B. K. (1998) Amelioration by cyclosporin A of brain damage in transient forebrain ischemia in the rat. *Brain Res.* **812,** 216-226

26. Yoshimoto, T., and Siesjo, B. K. (1999) Posttreatment with the immunosuppressant cyclosporin A in transient focal ischemia. *Brain Res.* **839,** 283-291

27. Szewczyk, A., and Wojtczak, L. (2002) Mitochondria as a pharmacological target. *Pharmacol. Rev.* **54,** 101-127

28. Green, D. R., and Reed, J. C. (1998) Mitochondria and apoptosis. *Science* **281,** 1309-1312

29. Martinou, J. C., and Green, D. R. (2001) Breaking the mitochondrial barrier. *Nat. Rev. Mol. Cell Biol.* **2,** 63-67

30. Liu, X., Kim, C. N., Yang, J., Jemmerson, R., and Wang, X. (1996) Induction of apoptotic program in cell-free extracts: requirement for dATP and cytochrome c. *Cell* **86,** 147-157

31. Bernardi, P., Petronilli, V., Di Lisa, F., and Forte, M. (2001) A mitochondrial perspective on cell death. *Trends Biochem. Sci.* **26,** 112-117

32. Qian, T., Herman, B., and Lemasters, J. J. (1999) The mitochondrial permeability transition mediates both necrotic and apoptotic death of hepatocytes exposed to Br-A23187. *Toxicol. Appl. Pharmacol.* **154,** 117-125

33. Halestrap, A. P., McStay, G. P., and Clarke, S. J. (2002) The permeability transition pore complex: another view. *Biochimie* **84,** 153-166

34. Zamzami, N., Marchetti, P., Castedo, M., Hirsch, T., Susin, S. A., Masse, B., and Kroemer, G. (1996) Inhibitors of permeability transition interfere with the disruption of the mitochondrial transmembrane potential during apoptosis. *FEBS Lett.* **384,** 53-57

35. Zoratti, M., and Szabo, I. (1994) Electrophysiology of the inner mitochondrial membrane. *J. Bioenerg. Biomembr.* **26,** 543-553

36. Longa, E. Z., Weinstein, P. R., Carlson, S., and Cummins, R. (1989) Reversible middle cerebral artery occlusion without craniectomy in rats. *Stroke* **20,** 84-91

37. Belayev, L., Alonso, O. F., Busto, R., Zhao, W., and Ginsberg, M. D. (1996) Middle cerebral artery occlusion in the rat by intraluminal suture. Neurological and pathological evaluation of an improved model. *Stroke* **27,** 1616-1622

38. Loupatatzis, C., Seitz, G., Schonfeld, P., Lang, F., and Siemen, D. (2002) Single-channel currents of the permeability transition pore from the inner mitochondrial membrane of rat liver and of a human hepatoma cell line. *Cell Physiol. Biochem.* **12,** 269-278

39. Ichas, F., and Mazat, J. P. (1998) From calcium signaling to cell death: two conformations for the mitochondrial permeability transition pore. Switching from low- to high-conductance state. *Biochim. Biophys. Acta* **1366,** 33-50

40. Fournier, N., Ducet, G., and Crevat, A. (1987) Action of cyclosporine on mitochondrial calcium fluxes. *J. Bioenerg. Biomembr.* **19,** 297-303

41. Crompton, M., Ellinger, H., and Costi, A. (1988) Inhibition by cyclosporin A of a Ca2+-dependent pore in heart mitochondria activated by inorganic phosphate and oxidative stress. *Biochem. J.* **255,** 357-360

42. Kowaltowski, A. J., Castilho, R. F., and Vercesi, A. E. (2001) Mitochondrial permeability transition and oxidative stress. *FEBS Lett.* **495,** 12-15

43. Siemen et al. (2002) The dopamine-D2-receptor agonist pramipexole dose-dependently blocks the Ca2+-triggered permeability transition of mitochondria. *Rest. Neuro. Neurosci.* **20,** 275-276

44. Lorenz, P., Roychowdhury, S., Engelmann, M., Wolf, G., and Horn, T. F. W.(2003) Oxyresveratrol and resveratrol are potent antioxidants and free radical scavengers: effect on nitrosative and oxidative stress derived from microglial cells. *Nitric Oxide* **9,** 64-76

45. Wang, X. (2001) The expanding role of mitochondria in apoptosis. *Genes Dev.* **15,** 2922-2933

46. Reichert, S. A., Kim-Han, J. S., and Dugan, L. L. (2001) The mitochondrial permeability transition pore and nitric oxide synthase mediate early mitochondrial depolarization in astrocytes during oxygen-glucose deprivation. *J. Neurosci.* **21,** 6608-6616

47. Smaili, S. S., and Russell, J. T. (1999) Permeability transition pore regulates both mitochondrial membrane potential and agonist-evoked Ca2+signals in oligodendrocyte progenitors. *Cell Calcium* **26,** 121-130

48. Fiskum, G., Murphy, A. N., and Beal, M. F. (1999) Mitochondria in neurodegeneration: acute ischemia and chronic neurodegenerative diseases. *J. Cereb. Blood Flow Metab.* **19,** 351-369

49. Siesjo, B. K. (1992) Pathophysiology and treatment of focal cerebral ischemia. Part I: Pathophysiology. *J. Neurosurg.* **77,** 169-184

50. Siesjo, B. K. (1985) Acid-base homeostasis in the brain: physiology, chemistry, and neurochemical pathology. *Prog. Brain Res.* **63,** 121-154

51. Halestrap, A. P. (1999) The mitochondrial permeability transition: its molecular mechanism and role in reperfusion injury. *Biochem. Soc. Symp.* **66,** 181-203

52. Hansen, A. J., and Zeuthen, T. (1981) Extracellular ion concentrations during spreading depression and ischemia in the rat brain cortex. *Acta Physiol. Scand.* **113,** 437-445

53. Back, T., Hoehn, M., Mies, G., Busch, E., Schmitz, B., Kohno, K., and Hossmann, K. A. (2000) Penumbral tissue alkalosis in focal cerebral ischemia: relationship to energy metabolism, blood flow, and steady potential. *Ann. Neurol.* **47,** 485-492

54. Piantadosi, C. A., and Zhang, J. (1996) Mitochondrial generation of reactive oxygen species after brain ischemia in the rat. *Stroke* **27,** 327-331

55. Simon, R. P., Griffiths, T., Evans, M. C., Swan, J. H., and Meldrum, B. S. (1984) Calcium overload in selectively vulnerable neurons of the hippocampus during and after ischemia: an electron microscopy study in the rat. *J. Cereb. Blood Flow Metab.* **4,** 350-361

56. Matsumoto, S., Isshiki, A., Watanabe, Y., and Wieloch, T. (2002) Restricted clinical efficacy of cyclosporin A on rat transient middle cerebral artery occlusion. *Life Sci.* **72,** 591-600

57. Matsumoto, S., Friberg, H., Ferrand-Drake, M., and Wieloch, T. (1999) Blockade of the mitochondrial permeability transition pore diminishes infarct size in the rat after transient middle cerebral artery occlusion. *J. Cereb. Blood Flow Metab.* **19,** 736-741

58. Nakatsuka, H., Ohta, S., Tanaka, J., Toku, K., Kumon, Y., Maeda, N., Sakanaka, M., and Sakaki, S. (1999) Release of cytochrome c from mitochondria to cytosol in gerbil hippocampal CA1 neurons after transient forebrain ischemia. *Brain Res.* **849,** 216-219

59. Liu, W., Liu, R., Chun, J. T., Bi, R., Hoe, W., Schreiber, S. S., and Baudry, M. (2001) Kainate excitotoxicity in organotypic hippocampal slice cultures: evidence for multiple apoptotic pathways. *Brain Res.* **916,** 239-248

60. Ferrand-Drake, M., Zhu, C., Gido, G., Hansen, A. J., Karlsson, J. O., Bahr, B. A., Zamzami, N., Kroemer, G., Chan, P. H., Wieloch, T., and Blomgren, K. (2003) Cyclosporin A prevents calpain activation despite increased intracellular calcium concentrations, as well as translocation of apoptosis-inducing factor, cytochrome c and caspase-3 activation in neurons exposed to transient hypoglycemia. *J. Neurochem.* **85,** 1431-1442

61. Jiang, D., Sullivan, P. G., Sensi, S. L., Steward, O., and Weiss, J. H. (2001) Zn(2+) induces permeability transition pore opening and release of pro-apoptotic peptides from neuronal mitochondria. *J. Biol. Chem.* **276,** 47524-47529

62. Cassarino, D. S., Parks, J. K., Parker, W. D., Jr., and Bennett, J. P., Jr. (1999) The parkinsonian neurotoxin MPP+ opens the mitochondrial permeability transition pore and releases cytochrome c in isolated mitochondria via an oxidative mechanism. *Biochim. Biophys. Acta* **1453,** 49-62

63. Andreyev, A., and Fiskum, G. (1999) Calcium induced release of mitochondrial cytochrome c by different mechanisms selective for brain versus liver. *Cell Death Differ.* **6,** 825-832

64. Li, P., Nijhawan, D., Budihardjo, I., Srinivasula, S. M., Ahmad, M., Alnemri, E. S., and Wang, X. (1997) Cytochrome c and dATP-dependent formation of Apaf-1/caspase-9 complex initiates an apoptotic protease cascade. *Cell* **91,** 479-489

65. Kunduzova, O. R., Escourrou, G., Seguelas, M. H., Delagrange, P., De La Farge, F., Cambon, C., and Parini, A. (2003) Prevention of apoptotic and necrotic cell death, caspase-3 activation, and renal dysfunction by melatonin after ischemia/reperfusion. *FASEB J.* **17,** 872-874

66. Shen, Y. X., Xu, S. Y., Wei, W., Wang, X. L., Wang, H., and Sun, X. (2002) Melatonin blocks rat hippocampal neuronal apoptosis induced by amyloid beta-peptide 25-35. *J Pineal Res.* **32,** 163-167

67. Yoo, Y. M., Yim, S. V., Kim, S. S., Jang, H. Y., Lea, H. Z., Hwang, G. C., Kim, J. W., Kim, S. A., Lee, H. J., Kim, C. J., Chung, J. H., and Leem, K. H. (2002) Melatonin suppresses NO-induced apoptosis via induction of Bcl-2 expression in PGT-beta immortalized pineal cells. *J. Pineal Res.* **33,** 146-150

68. Harms, C., Lautenschlager, M., Bergk, A., Freyer, D., Weih, M., Dirnagl, U., Weber, J. R., and Hortnagl, H. (2000) Melatonin is protective in necrotic but not in caspase-dependent, free radical-independent apoptotic neuronal cell death in primary neuronal cultures. *FASEB J.* **14,** 1814-1824

69. Krohn, A. J., Wahlbrink, T., and Prehn, J. H. (1999) Mitochondrial depolarization is not required for neuronal apoptosis. *J. Neurosci.* **19,** 7394-7404

70. Hortnagl, H., Berger, M. L., Reither, H., and Hornykiewicz, O. (1991) Cholinergic deficit induced by ethylcholine aziridinium (AF64A) in rat hippocampus: effect on glutamatergic systems. *Naunyn Schmiedebergs Arch. Pharmacol.* **344,** 213-219

71. Chung, S.-Y., and Han, S.-H. (2003) Melatonin attenuates kainic acid-induced hippocampal neurodegeneration and oxidative stress through microglial inhibition. *J. Pineal Res.* **34,** 95-102

72. Cuzzocrea, S., Costantino, G., Gitto, E., Mazzon, E., Fulia, F., Serraino, I., Cordaro, S., Barberi, I., De Sarro, A., and Caputi, A. P. (2000) Protective effects of melatonin in ischemic brain injury. *J. Pineal Res.* **29,** 217-227

73. Kilic, E., Ozdemir, Y. G., Bolay, H., Kelestimur, H., and Dalkara, T. (1999) Pinealectomy aggravates and melatonin administration attenuates brain damage in focal ischemia. *J. Cereb. Blood Flow Metab.* **19,** 511-516

74. Reiter, R. J. (1992) The ageing pineal gland and its physiological consequences. *Bioessays* **14,** 169-175

75. Pennartz, C. M., de Jeu, M. T., Bos, N. P., Schaap, J., and Geurtsen, A. M. (2002) Diurnal modulation of pacemaker potentials and calcium current in the mammalian circadian clock. *Nature* **416,** 286-290

Received October 16, 2003; accepted February 2, 2004.

Fig. 1

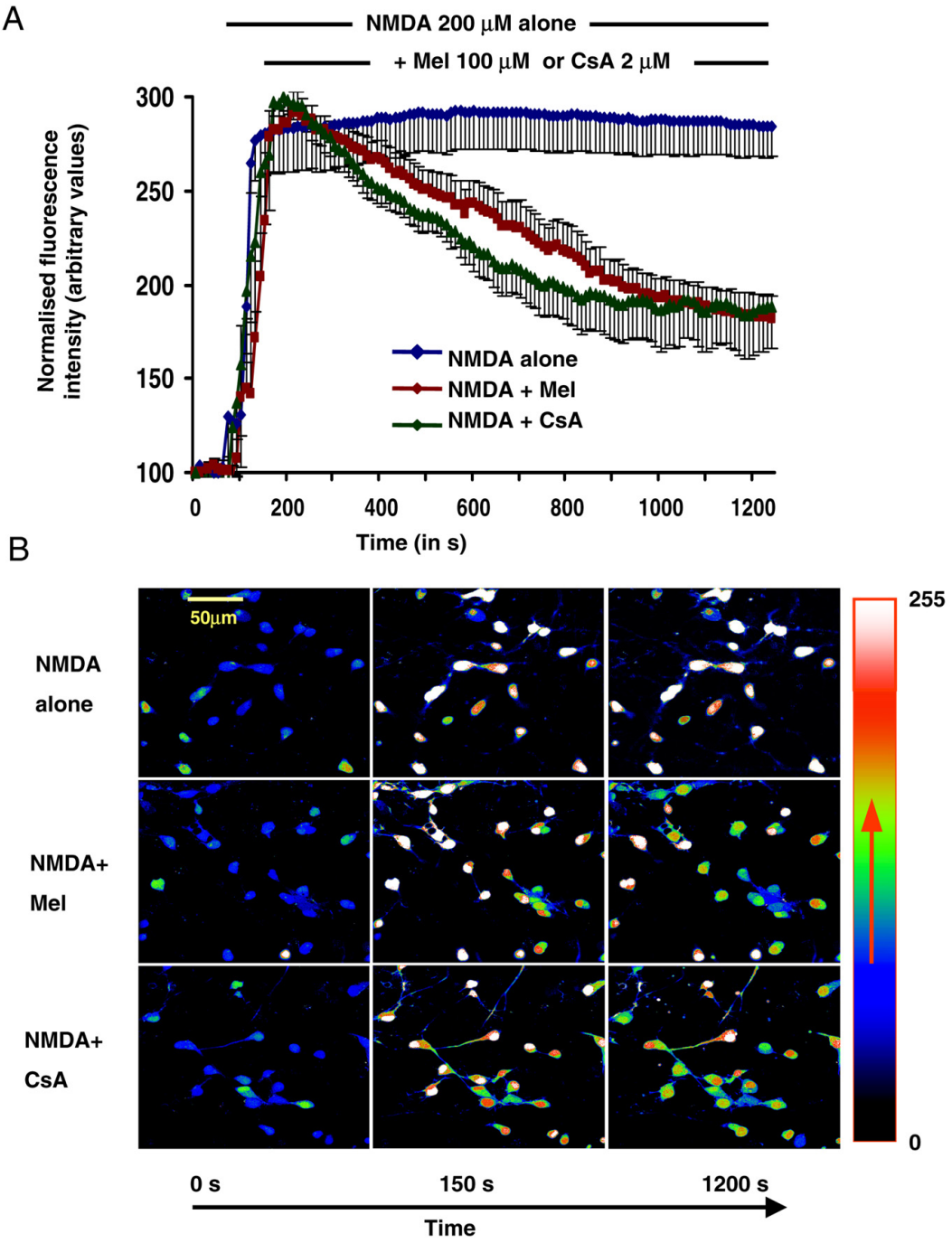

Figure 1. Melatonin decreases NMDA-induced intracellular calcium levels. Neuronal cultures were loaded with the Ca^{2+}-sensitive fluorochrome fluo-4, and time series of confocal images were recorded to monitor fluorescence intensities. NMDA was applied alone (200 μM, blue line) or together with CsA (2 μM, green line) or melatonin (100 μM, red line). Black lines above graph are duration of treatments. ***A***) Depicted are average fluorescence intensity traces of different treatment groups reflecting intracellular Ca^{2+} levels. Traces were obtained by analyzing average pixel fluorescence intensity within boxes drawn over single cell somata for each image of time series. NMDA alone shows a rise in $[Ca^{2+}]_c$ in neurons that sustained at a plateau level throughout continuous NMDA application. Both melatonin and CsA decreased the sustained rise in $[Ca^{2+}]_c$ in NMDA-stimulated neurons. Normalized data are means ± SE; n = 5 cultures for each group. ***B***) Representative images of fluo-4 loaded cultures. Left column is baseline fluorescence before NMDA application, and the 2 other columns show elevated fluorescence during NMDA exposure. Upper row (NMDA alone) is sustained rise in $[Ca^{2+}]_c$ after NMDA application. Middle row (NMDA + Mel) indicates that although these neurons displayed an initial high $[Ca^{2+}]_c$ level after NMDA exposure onset, fluorescence decreased in presence of melatonin. Lower panel of images is a similar effect of CsA on the NMDA-induced $[Ca^{2+}]_c$ level as seen with melatonin.

Fig. 2

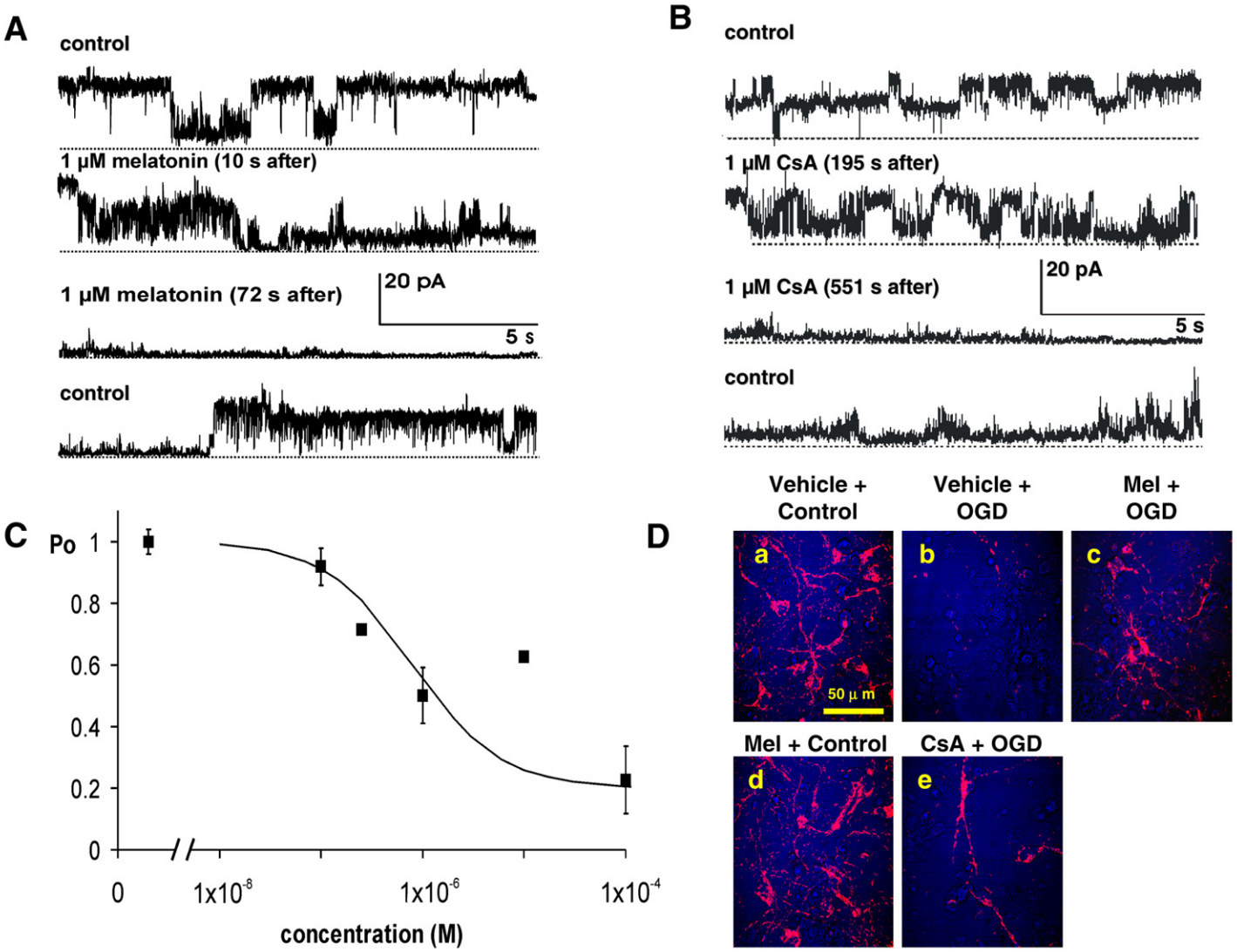

Figure 2. Melatonin dose-dependently blocks the mtPTP currents in mitoplast membrane patches. ***A*****)** Effect of melatonin on single channel currents recorded from the mtPTP of mitoplast membrane. Shown are representative traces of mtPTP activity with a representative 1 µM melatonin application. Baseline mtPTP activity (control, 1st trace) was blocked by 1µM melatonin (2nd and 3rd trace, at 10 s and 72 s, respectively, after switching to melatonin), which was reversible (4th trace, after switching to control). Dotted lines give zero-current level; holding potential (E_h) +20 mV. ***B*****)** Representative traces of mtPTP activity (control, 1st trace), with CsA application (2nd and 3rd trace) and after switching back to control solution (4th trace). ***C*****)** Concentration-response curve for normalized open propability (Po) under influence of melatonin at E_h = +20 mV. Po was estimated by all-point analysis of the single channel data in 1 min segments from each experiment, starting 1 min after addition of melatonin. Mean Po were calculated from 2 independent experiments at each concentration. Data are means ± SE, and curve was calculated by means of the Hill equation (Hill coefficient: 1) with a half-maximum P_o (IC_{50}) at 0.8 µM. ***D*****)** Melatonin preserves rate of TMRM uptake after OGD. Representative pictures showing an overlay of a phase contrast image and an image of TMRM fluorescence. Red color shows TMRM-loaded mitochondria, indicating an intact $\Delta\Psi_m$. Images were obtained after cultures were subjected to 3 h OGD followed by 30 min oxygen-glucose resupply. TMRM was added to culture medium at time of oxygen-glucose resupply. ***a*****)** Control culture with strongly stained mitochondria-like structures. In ***b***, an OGD-treated culture is shown that has almost completely lost the ability to take up TMRM into mitochondria, indicating a loss of $\Delta\Psi_m$. OGD-subjected cultures (***c***) that contained melatonin (100 µM) in medium, in contrast, retained the capacity to load TMRM. Melatonin alone (***d***) did not alter TMRM uptake in control cultures. Analoguous to melatonin, a treatment with 2 µM CsA (***e***) also prevented loss of $\Delta\Psi_m$ as indicated by mitochondrial uptake of TMRM in some cells.

Fig. 3

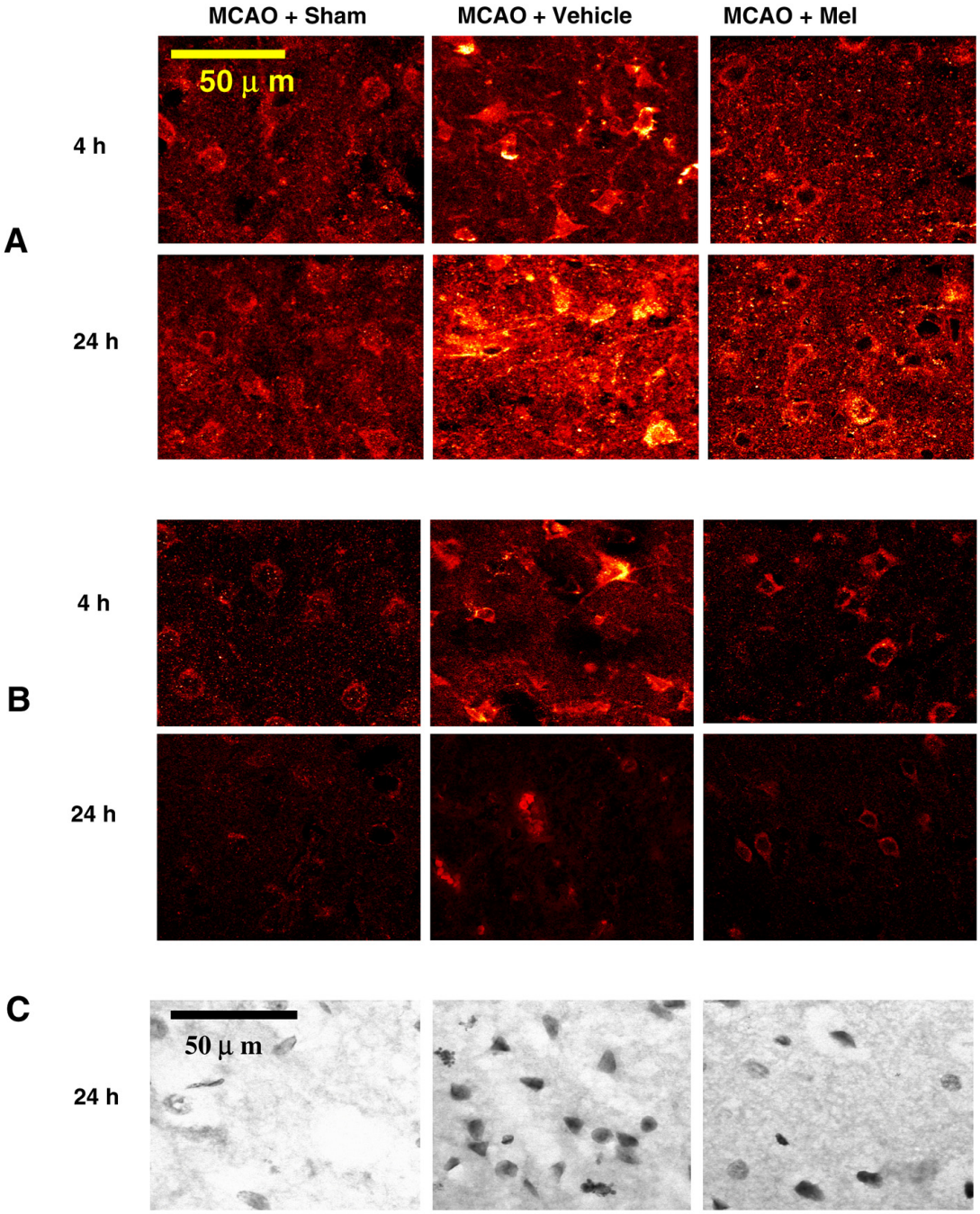

Figure 3. ***A*) Cytosolic cyt c immunoreactivity is decreased in MCAO brain tissue on melatonin treatment.** Representative pictures of cyt c immunostaining in MCA-supplied cortex obtained at 4 (upper panel) or 24 h (lower panel). No specific cytosolic immunostaining is seen in "Sham + Vehicle" rats, both at 4 and 24 h. Characteristic cyt c labeling in cytosol of cells is observed after 4 and 24 h in the "MCAO + Vehicle" rats. After 24 h, staining is seen in intercellular spaces, indicating the presence of cell debris. Melatonin treatment greatly reduces cytosolic cyt c immunostaining in "MCAO + Mel" rats both at 4 h as well as 24 h. ***B*)** MCAO-induced caspase-3 immunoreactivity is reduced by melatonin. Corresponding caspase-3 immunofluorescence of MCA-supplied cortex in sections adjacent to those seen in ***A***. No activation of caspase-3 is seen in "Sham + Vehicle" rats, whereas in vehicle-treated MCAO rats, most of the cells show an increased caspase-3 immunostaining at 4 h. At 24 h, an increased and patchy caspase-3 immunostaining is seen in "MCAO + Vehicle" rats. Melatonin treatment decreases caspase-3 activation both at 4 and 24 h after ischemia "MCAO + Mel" rats. ***C*)** Melatonin protects against MCAO-induced DNA fragmentation. Images are of apostain-labeled cortices, indicating the presence of apoptotic ssDNA. In "Sham + Vehicle" rats, no staining is observed while in "MCAO + Vehicle" rats, most of cells are apostain labeled. Darkly stained cells are shrunken and have a characteristic apoptotic-like appearance. Melatonin decreased number of apopstain-positive cells in "MCAO + Mel" rats.

Fig. 4

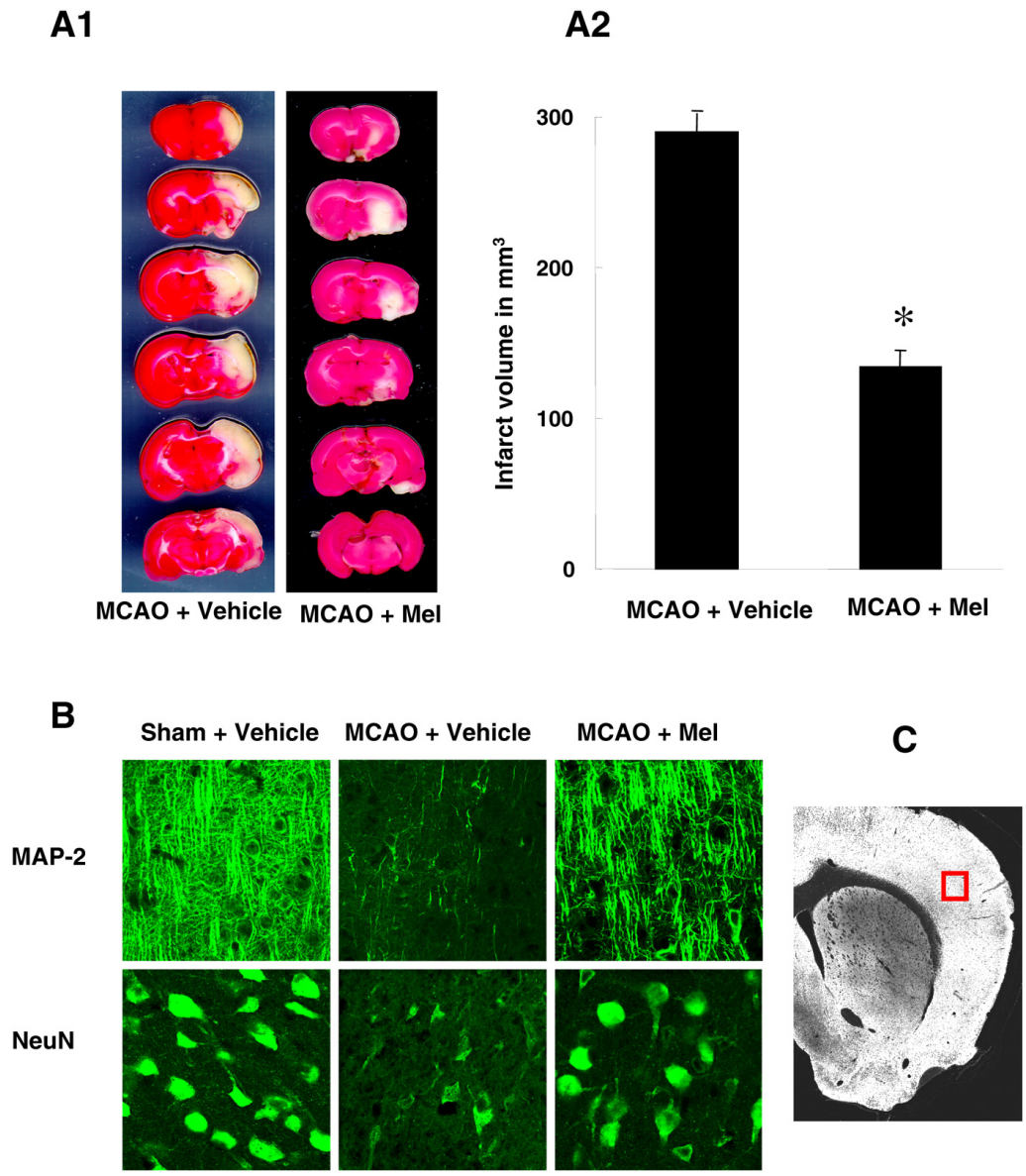

Figure 4. Melatonin reduces infarct volume. ***A1*****)** TTC-stained coronal sections from representative animals that received either vehicle (10% ethanol) or melatonin (10 mg/kg ip) both at time of occlusion as well as at time of reperfusion. Animals were euthanized 3 days after occlusion. Infarcts are observed as pale regions involving striatum and overlying cortex. Note that infarct area in melatonin-treated animal is substantially reduced. ***A2*****)** Statistical analysis of infarct volume. Reproducible infarct volumes are observed in "MCAO + Vehicle" rats subjected to 2 h occlusion followed by 3 days reperfusion. Melatonin significantly reduced infarct volume in "MCAO + Mel" (*P<0.05; n=10). Data are expressed as mm^3 and are means ± SE. ***B*****)** MAP-2 and NeuN immunostaining. Upper panel of pictures is MAP-2 immunostaining in sham-operated, vehicle-treated and melatonin-treated rats, subjected to 2 h occlusion followed by 24 h reperfusion. Neurons in "Sham + Vehicle" rats have an extensive array of branching dendrites and well-defined somta stained for MAP-2. A loss of both somatic and dendritic MAP-2 labeling is observed in "MCAO + Vehicle" rats at 24 h after reperfusion. Melatonin treatment prevented loss of MAP-2 staining in "MCAO + Mel" rats. Lower panel is NeuN immunostaining of sections from same groups as shown in upper panel. In "Sham + Vehicle" rats, a dense pattern of NeuN-positive cells is observed. In "MCAO + Vehicle" rats, NeuN-positive cells are almost completely lost at 24 h after reperfusion. Melatonin preserved NeuN-positive cells in ischemic tissue of the "MCAO + Mel" group. ***C*****)** Area of analysis: for microscopic analysis of different antigens a location of the cortex was chosen that consistently showed lesions in "MCAO + Vehicle" group. Image depicts a representative section selected by anatomical landmarks like the shape of commissura anterior. Inserted box is observation area.